

# ASF radiometric terrain corrected products

## Algorithm Theoretical Basis Document

---

ASF engineering

### ABSTRACT

This document provides the theoretical background of the algorithms and processing flows used for the generation of terrain corrected products processed at the Alaska Satellite Facility.



## Document preparation

The document was prepared with contributions from  
Rudi Gens

## Document change log

| Revision  | Date       | Page | Change Description                         | Reason for change |
|-----------|------------|------|--|-------------------|
| 1.0 Draft | 07/01/2014 | all  | Initial Draft                              |                   |
| 1.1       | 01/15/2015 | all  | More detailed description of the algorithm |                   |
| 1.2       | 06/01/2015 | all  | Added more detail on the processing flow   |                   |



## Table of Contents

|  |    |
|--|----|
| Document preparation.....                | 2  |
| Document change log .....                | 2  |
| Document structure .....                 | 4  |
| 1 Introduction and scope.....            | 5  |
| 2 Background.....                        | 5  |
| 2.1 SAR images.....                      | 5  |
| 2.2 Calibration.....                     | 5  |
| 2.3 Digital elevation models.....        | 7  |
| 3 Radiometric terrain correction .....   | 9  |
| 4 Processing flow .....                  | 11 |
| 4.1 Co-registration .....                | 12 |
| 4.2 Radiometric terrain correction ..... | 12 |
| 4.3 Product resolutions.....             | 14 |
| 4.4 Product generation .....             | 15 |
| References .....                         | 16 |



## Document structure

The document is structured as follows:

Chapter 1 introduces the structure and scope of the document.

Chapter 2 provides background information about SAR imagery, calibration, and digital elevation models.

Chapter 3 reviews the theoretical background of radiometric terrain correction.

Chapter 4 shows the processing flow for generating terrain corrected products. Details are provided about co-registration, the radiometric terrain correction and products generated.



## 1 Introduction and scope

The side-looking geometry of SAR imagery leads to geometric and radiometric distortions. This causes foreshortening, layover, shadowing, and radiometric variations due to the slope that make any further analysis difficult (Shimada, 2010).

Radiometric terrain correction improves backscatter estimates that can be used as input for applications such as the monitoring of deforestation, land-cover classification, and delineation of wet snow-covered areas (Small, 2011).

This Algorithm Theoretical Basis Document (ATBD) describes the basic algorithms of radiometric terrain correction using the Gamma Remote Sensing software.

The document will not describe the product specification, data format, and product planning. It will not provide any details of the implementation of the algorithms used.

## 2 Background

### 2.1 SAR images

The primary data source for generating geometrically and radiometrically corrected data products is the PALSAR imagery acquired during the ALOS mission (2006 to 2011). The terrain correction products are generated for all FBS, FBD, and PLR beam modes. They include all available beam modes for dual-pol and quad-pol data. Any wide-beam data, as well as direct downlink direct source network (DSN) data, directly acquired by the Alaska Satellite Facility at reduced resolution, are not terrain corrected.

### 2.2 Calibration

The objective of the calibration of SAR data is to provide imagery in which the pixel values can be directly related to the radar backscatter of the scene. It allows for quantitative analysis of the imagery and comparison between images.

In order to derive geophysical parameters from SAR data, Freeman (1992) established calibration requirements. The absolute calibration needs to be  $\pm 1$  dB with the long-term relative calibration  $\pm 0.5$  dB and the short-term relative calibration greater than 0.5 dB.

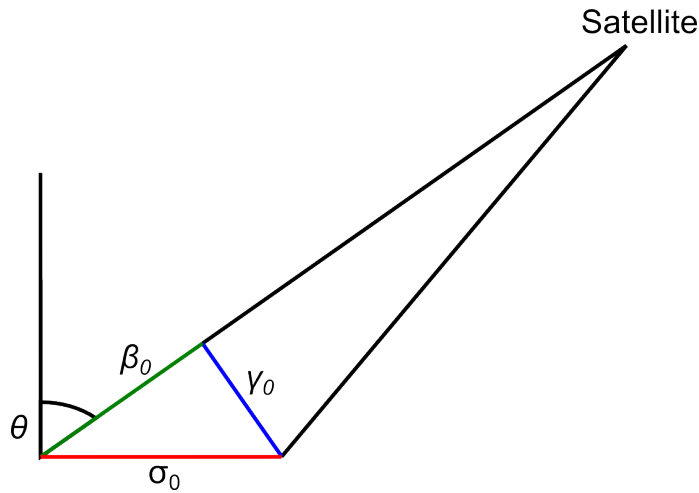


Figure 1: Calibration geometry

Calibrating a SAR image is the process of converting a linear amplitude image into a radiometrically calibrated power image. The input image is in units of digital numbers (DNs), whereas the output image is in units of  $\beta_0$ ,  $\gamma_0$ , or  $\sigma_0$ , which is the ratio of the power that comes back from a patch of ground to power sent to the patch of ground (Figure 1).

The application requirements will help determine which of these calibration units to choose. Scientists are generally interested

in quantitative measurements that are referenced to the ground, i.e. they work with  $\sigma_0$  values. For calibration purposes  $\gamma_0$  values are preferred because they are equally spaced. Finally, system design engineers choose to work with  $\beta_0$  values, because these values are independent from the observed terrain. Converting values from the  $\sigma_0$  generated in the terrain correction process to  $\beta_0$  and  $\gamma_0$  requires the incidence angle  $\theta$ :

$$\gamma_0 = \frac{\sigma_0}{\cos \theta}, \beta_0 = \frac{\sigma_0}{\sin \theta} \quad (1)$$

Shimada *et al.* (2009) summarized their assessment of the radiometric and geometric calibration of ALOS PALSAR data using two methods to determine the calibration factor relating the DN's to normalized radar cross section (NRCS). A corner reflector analysis compares actual point target analysis measurements with the theoretical radar cross section (RCS). Alternatively, data acquired over the Amazon rainforest are assumed to have a constant  $\gamma_0$  value of -6.5 dB (Shimada, 2005).

The NRCS is calculated using the following equation (Shimada *et al.*, 2009):

$$\sigma_{1.1 \text{ product}}^0 = 10 \log_{10}(I^2 + Q^2) + \text{CF} - \text{A} \quad (2)$$

with the real (I) and imaginary (Q) parts of the level 1.1 single look complex product, the calibration factor (CF), and the conversion factor (A) of 32.0. The analysis determined a constant CF of -83.0 dB that appeared to be stable over time. Shimada *et al.* (2009) reported a radiometric accuracy of 0.76 dB using corner reflectors and 0.22 dB from the Amazon forest

data. They concluded that the accuracy and image quality is sufficient to use ALOS PALSAR data for operationally monitoring deforestation and surface deformation.

### 2.3 Digital elevation models

The correction of the geometric distortions as well as the related radiometry adjustment of SAR imagery requires the use of digital elevation models (DEMs). The accuracy of a terrain corrected result is directly related to the quality of the DEM.

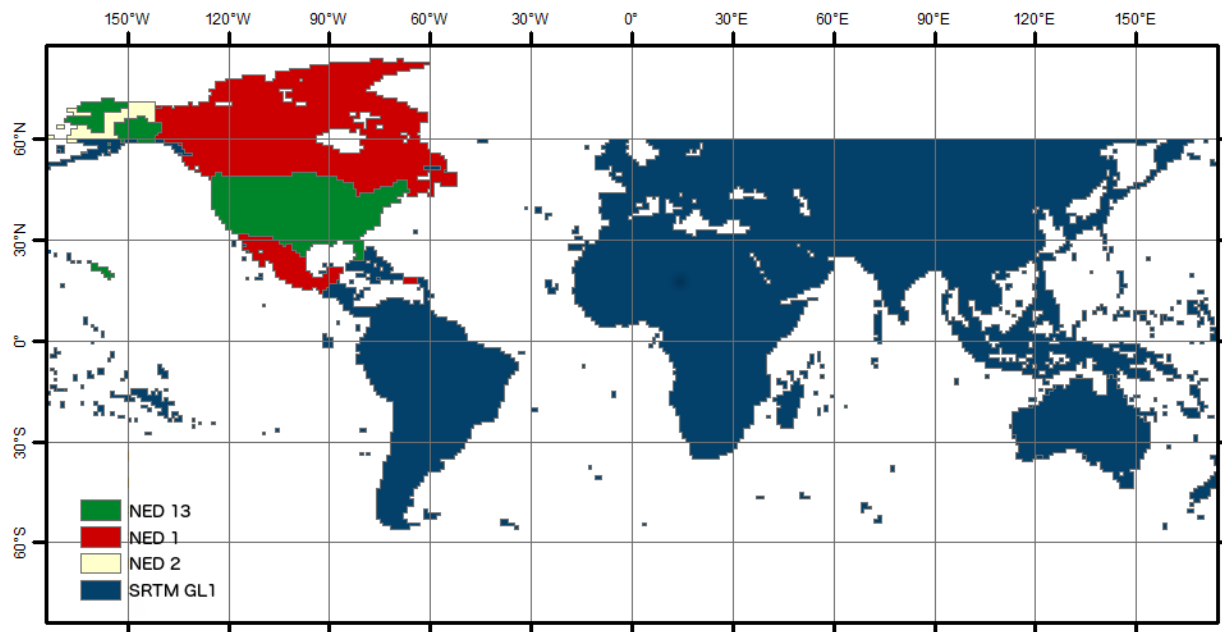


**Figure 2: Four different sources of DEMs are used for the terrain correction. Note high resolution DEMs are not available for Greenland, Eurasia above 60 degrees northern latitude, and Antarctica.**

Figure 2 shows the coverage of DEMs used for the terrain correction, provided by the United States Geological Survey (USGS). The Shuttle Radar Topography Mission (SRTM) data is globally available at a resolution of 30 m between 60 degrees northern and southern latitude. North America is covered by a variety of digital elevation models. For Canada and Mexico a National Elevation Dataset (NED) at a resolution of 1 arc-second is used. Alaska is generally covered with NED 2 arc-second resolution data as well as SRTM data at 30 m below 60 degrees northern latitude. The USGS provided data for some parts of Alaska and the contiguous United States (CONUS) at a 1/3 arc-second level.



The SRTM GL1 data showed a number of artifacts that needed to be corrected. In order to detect the anomalies, the slope to the neighboring pixel was calculated in both image direction. Any absolute local slope greater than 400 m was marked as anomaly. The spikes and holes forming the anomalies in the DEM were removed by adaptive triangulation using the Quick Terrain Modeler software.

The accuracy of these various DEM sources was analyzed by Gesch *et al.* (2014), comparing the DEM with reference data in the form of geodetic control points of the National Geodetic Survey (NGS). The results are summarized in Table 1.

| DEM Source           | RMSE [m] |
|----------------------|----------|
| CONUS 1/3 arc-second | 1.55     |
| CONUS 1 arc-second   | 2.44     |
| Alaska 2 arc-second  | 4.85     |
| Canada 1 arc-second  | 3.64     |
| Mexico 1 arc-second  | 6.74     |

**Table 1: Absolute vertical accuracy of the various NED sources (Gesch *et al.*, 2014)**

The comparison of 1 arc-second NED with other large-area elevation datasets showed the following accuracies (Table 2):

| DEM Source       | RMSE [m] |
|------------------|----------|
| NED 1 arc-second | 1.84     |
| SRTM 30 m        | 4.01     |
| ASTER GDEM 30 m  | 8.68     |

**Table 2: Accuracy assessment of large-area elevation datasets (Gesch *et al.*, 2014)**

The DEMs are organized and assembled as virtual raster mosaics from which the necessary subsets are extracted that cover the relevant areas for the terrain correction. The DEM values are geoid corrected.



### 3 Radiometric terrain correction

Radiometric terrain correction addresses two aspects of adjusting the effects of side-looking geometry of SAR imagery. First, the geometric distortions are corrected by using a digital elevation model. Second, the brightness, or radiometry, is adjusted in the affected foreshortening and layover regions.

Small (2011) comprehensively reviewed the various techniques for radiometric terrain correction and concluded that the pixel-area integration approach is the most robust technique available to radiometrically normalize SAR imagery.

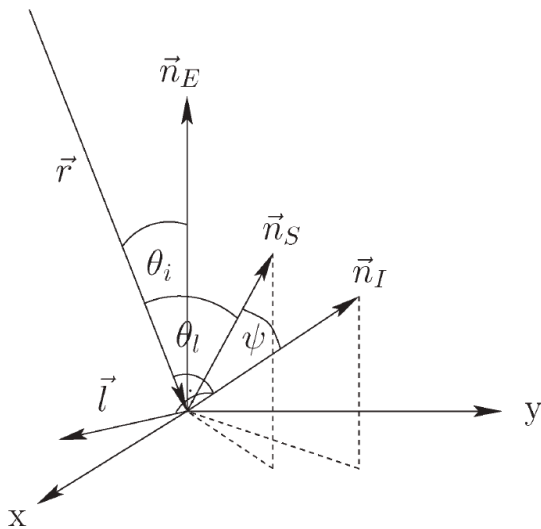


**Figure 3: Geometric relationships for angle-based simulations of illuminated area**  
(Source: Frey et al., 2013)

Figure 3 (Frey et al., 2013) provides the geometric definitions for the illuminated area.  $\vec{r}$  is the range vector in the line of sight.  $\vec{l}$  is pointing in the azimuth direction.  $\vec{n}_E$  is the ellipsoid normal vector.  $\vec{n}_I$  is the vector normal to the image plane, the normalized cross product of  $\vec{l}$  and  $\vec{r}$ .  $\vec{n}_S$  is the normalized surface normal vector.  $\theta_i$  is the ellipsoid-based incidence angle.  $\theta_l$  is the local incidence angle. Finally,  $\psi$  is the projection angle that relates the unit image area to the unit ground area when using the projection cosine approach.

The pixel-area integration for the radiometric normalization adjusts the brightness of the individual SAR image pixels, particularly in layover regions, by determining the actual area on the ground that the SAR signal was backscattered from. The average backscatter coefficient  $\sigma_0$  is calculated by

$$\sigma_0 = \beta_0 \frac{A_{\sigma_{\cos}}^0}{A_{\sigma_{pa}}^0}, \quad (3)$$

using the radar brightness  $\beta_0$ , the ellipsoid reference area  $A_{\sigma_{\cos}}^0$ , and the illuminated topographic pixel area  $A_{\sigma_{pa}}^0$  (Frey et al., 2013).

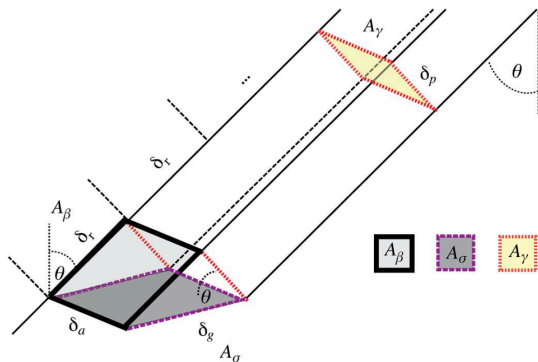


Figure 4: Normalization areas for SAR backscatter (Source: Small, 2011)

The radar brightness  $\beta_0$  is the ratio of the radar backscatter  $\beta$  and the reference area  $A_\beta$  (Small, 2011).

For a better approximation of area integral the digital elevation model is divided into rectangular regions that then subdivided into two triangular facets (Figure 5). The surface normal is defined for these triangular facets. Based on the geometry relative to the radar look vector (Figure 6), the projected pixel area of the facet is determined and added to the pixel-area map in range-Doppler coordinates.

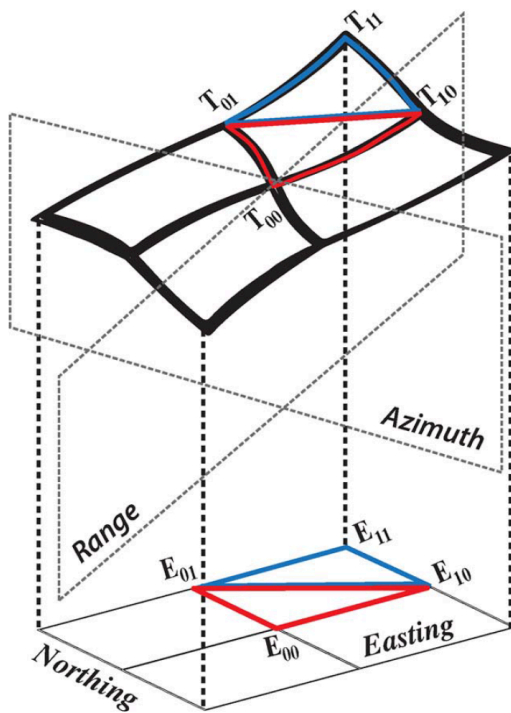


Figure 5: Digital height model facet neighborhood (Source: Small, 2011)

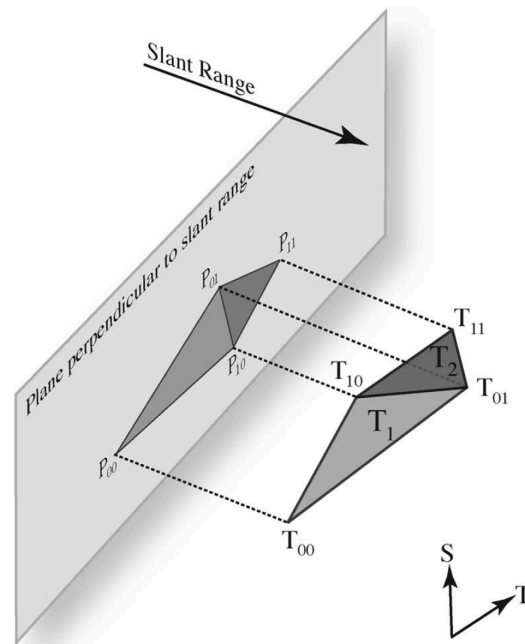


Figure 6: Projection of digital elevation facets into viewing plane (Source: Small, 2011)

In Gamma's implementation of this approach, summarized in Figure 7, each triangular facet is further divided into a number of rectangles that are then integrated into the correct range bin using the same surface normal defined for the triangle.

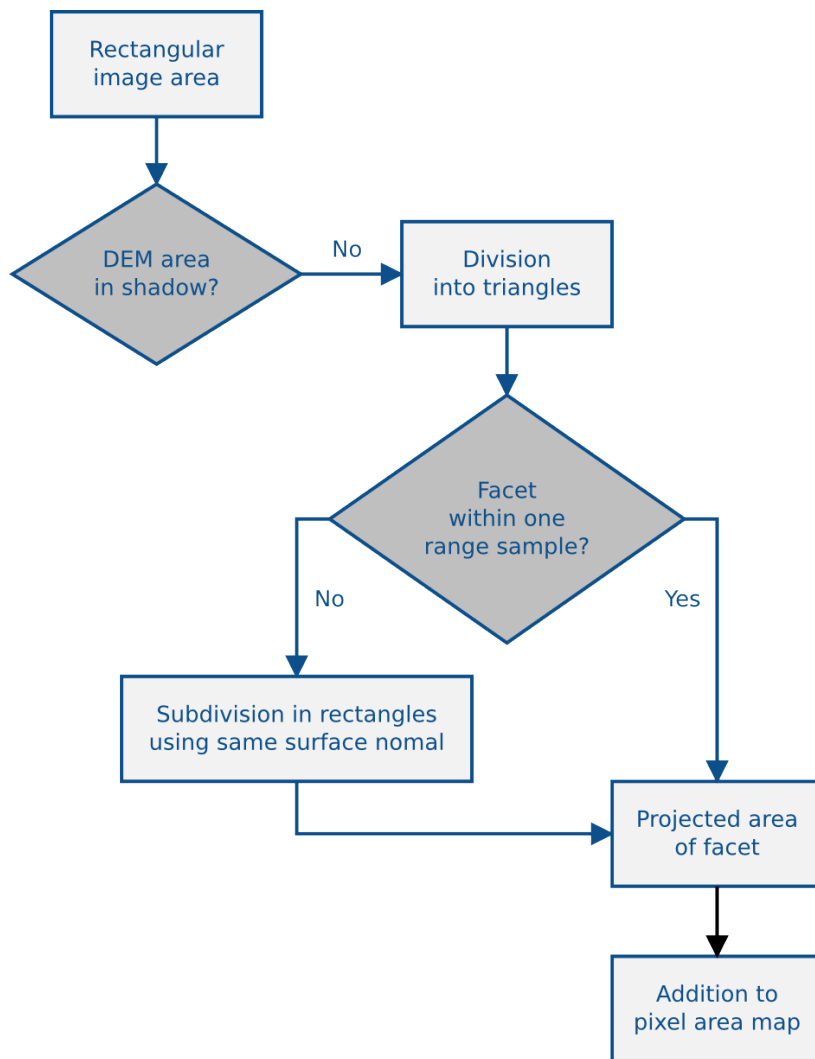


Figure 7: Processing flow for area integration calculation

## 4 Processing flow

The terrain corrected products are derived from ALOS PALSAR level 1.1 single look complex data, generated by the JAXA Sigma SAR processor (version 12.01) of the ALOS core software (release 6.07).

## 4.1 Co-registration

The geolocation quality of the terrain corrected product depends largely on the matching of the SAR image and the simulated image derived from the DEM during the co-registration.

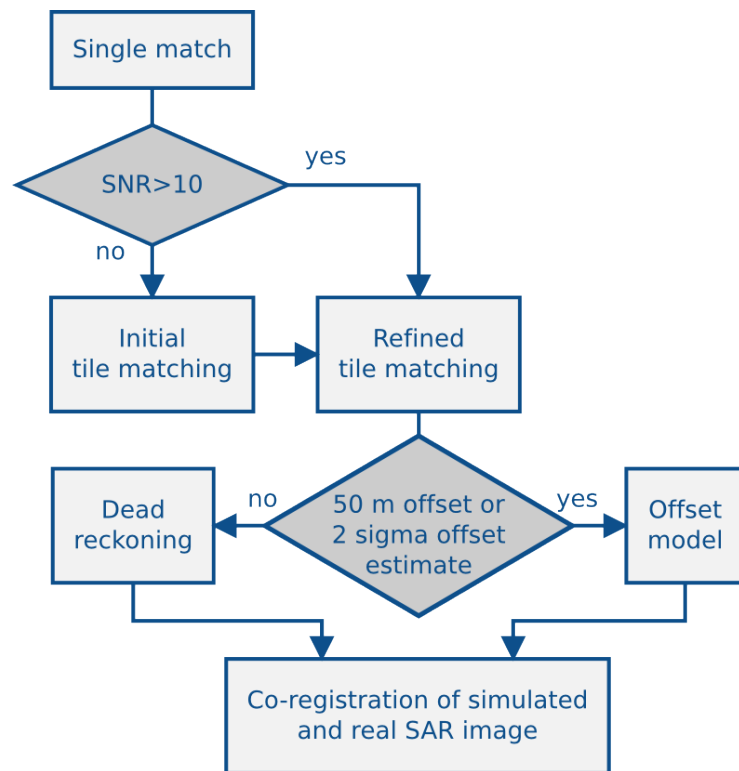


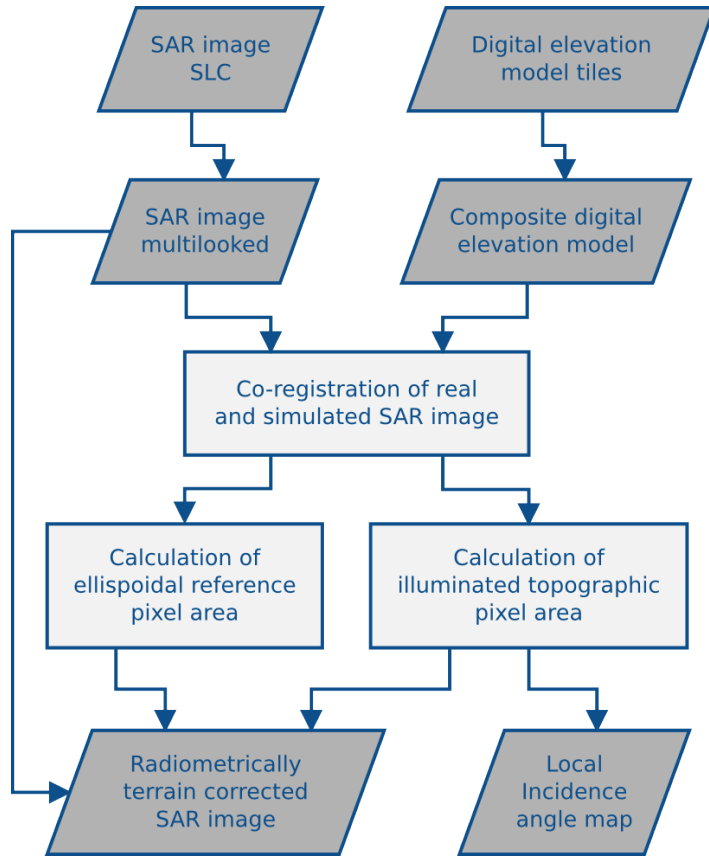
**Figure 8: Co-registration approach for the terrain correction**

Alternatively, when the refined tile matching meets or exceeds the SNR threshold the azimuth and range offsets are the input for determining a least-squares polynomial fit, using a singular value decomposition. The results of the offset model are then used to co-register the real and simulated SAR image.

## 4.2 Radiometric terrain correction

The radiometric terrain correction (outline in Figure 8) is performed entirely in slant range geometry.

Figure 7 summarizes the co-registration approach taken for the terrain correction. In order to determine initial offsets, a single match between real and simulated image is attempted. If the single match does not meet or exceed the signal-to-noise ratio (SNR) of 10 dB, tile matching on a coarse grid is performed. The initial offsets are then improved on a finer grid of tiles. Points that exceed a SNR of 10 dB are culled out. Otherwise, two criteria are applied to determine which processing option is executed: either an offset threshold of 50 m or an offset estimate of two standard deviations. If these criteria are not met, no offsets are applied. This approach, also called dead reckoning, relies entirely on the quality of the



First, the digital elevation model is projected into the slant range geometry so that a simulated SAR image can be derived. The correct number of azimuth looks is calculated as the ratio of ground range pixel sizes in azimuth ( $ypix$ ) and range, after range pixel size converted from slant range ( $xpix_{SR}$ ) to ground range ( $xpix_{GR}$ ) using the center incidence angle ( $incid$ ) provided in the metadata.

$$xpix_{GR} = \frac{xpix_{SR}}{\sin(incid)} \quad (4)$$

Based on the posting (12.5 m or 30 m) the range looks ( $looks_{range}$ ) and azimuth looks ( $looks_{azimuth}$ ) are calculated.

$$looks_{range} = int\left(\frac{posting}{xpix_{GR}+0.5}\right) \quad (5)$$

$$looks_{azimuth} = int\left(\frac{posting}{ypix+0.5}\right) \quad (6)$$

Figure 9: Processing flow of radiometric terrain correction

The adjustment of the radar brightness  $\beta^0$  is determined by multiplying it by the ratio of pixel area from the ellipsoidal reference  $A_\beta$  over the integrated pixel area  $A_\gamma$

$$\gamma_T^0 = \beta^0 \cdot \frac{A_\beta}{\int_{DHM} A_\gamma} \quad (7)$$

A side product of the illuminated topographic pixel area calculation is the local incidence angle map.

The inversion of the mapping function used to establish the relation between SAR geometry and the DEM in map projected space is used to terrain correct and geocode the radiometrically corrected SAR image.

### 4.3 Product resolutions

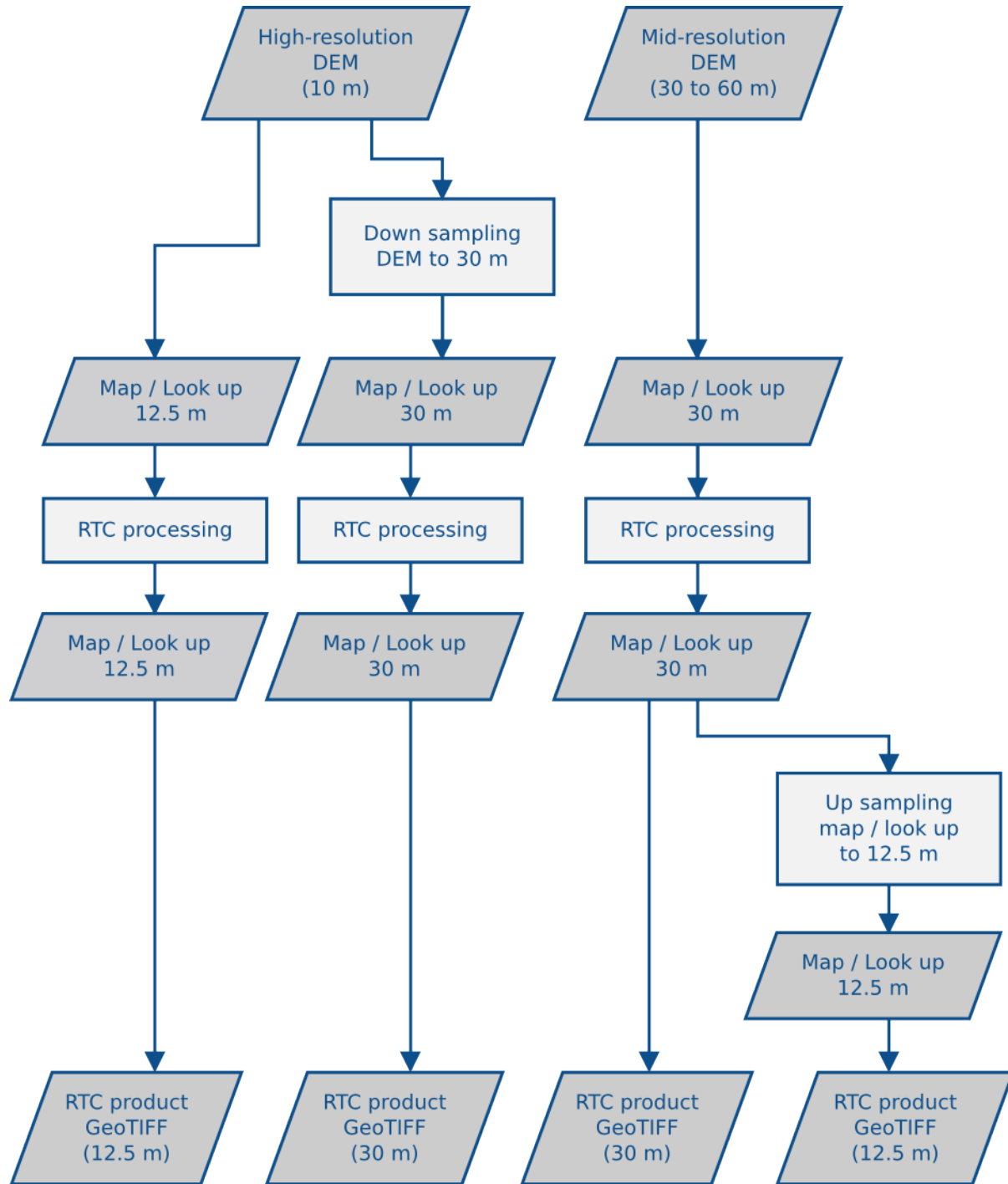


Figure 10: Processing flow for different DEM resolutions



Figure 10 summarizes the various processing flows for the different DEM resolutions. For the generation of the 30-m RTC product derived from high-resolution DEM, the input DEM is first down sampled from 10 m to 30 m posting before RTC processing is carried out. In order to produce a 12.5-m version from mid-resolution DEMs the 30-m RTC product is up sampled to a pixel size of 12.5 m, before it is exported to GeoTIFF format.

#### 4.4 Product generation

Depending on the availability of DEMs, the terrain correction products and supplemental information are provided at various resolutions as summarized in Table 3.

| DEM source | DEM resolution | RTC product | Reference DEM coverage |      | Layover/shadow mask |      | Incidence angle map |      |
|------------|----------------|-------------|------------------------|------|---------------------|------|---------------------|------|
|            |                |             | 12.5 m                 | 30 m | 12.5 m              | 30 m | 12.5 m              | 30 m |
| NED2       | 2 arc-second   | 12.5 m      | •                      |      |                     | •    |                     | •    |
|            |                | 30 m        |                        | •    |                     | •    |                     | •    |
| NED1       | 1 arc-second   | 12.5 m      | •                      |      |                     | •    |                     | •    |
|            |                | 30 m        |                        | •    |                     | •    |                     | •    |
| SRTM       | 30 m           | 12.5 m      | •                      |      |                     | •    |                     | •    |
|            |                | 30 m        |                        | •    |                     | •    |                     | •    |
| NED13      | 1/3 arc-second | 12.5 m      | •                      |      | •                   |      | •                   |      |
|            |                | 30 m        |                        | •    |                     | •    |                     | •    |

Table 3: Radiometric terrain correction (RTC) product specifications

RTC products are distributed at two resolutions. The RT1 products have a pixel size of 12.5 m and are generated from high-resolution (NED13) and mid-resolution (SRTM 30 m, NED1 and NED2) DEMs. The RT2 products are generated at a 30 m level for all available DEMs. Layover and shadow masks as well as incidence angle maps for mid-resolution DEMs are generated with a pixel size of 30 m. The supplementary products (reference DEM coverage, layover/shadow mask and incidence angle map) of 12.5 m resolution are also available for RT1 products derived from high-resolution. All products are terrain corrected at the native pixel size of the DEM that is used for the correction. No additional resampling is required.

All RTC products are geocoded to the Universal Transverse Mercator (UTM) projection and provided as floating-point power values in GeoTIFF format. The reference for the RTC products is pixel as point.

## References

- Freeman, A., 1992. SAR calibration: An overview. *IEEE Transactions of Geoscience and Remote Sensing*, **30**(6):1107-1121.
- Frey, O., Santoro, M., Werner, C.L. and Wegmüller, U., 2013. DEM-based SAR pixel-area estimation for enhanced geocoding refinement and radiometric normalization. *IEEE Geoscience and Remote Sensing Letters*, **10**(1):48-52.
- Gesch, D.B., Oimoen, M.J., and Evans, G.A., 2014. Accuracy assessment of the U.S. Geological Survey National Elevation Dataset, and comparison with other large-area elevation datasets - SRTM and ASTER. *U.S. Geological Survey Open-File Report 2014–1008*, 10 p.
- Shimada, M., 2005. Long-term stability of L-band normalized radar cross section of Amazon rainforest using the JERS-1 SAR. *Canadian Journal of Remote Sensing*, **31**(1):132-137.
- Shimada, M., Isoguchi, O., Tadono, R. and Isono, K., 2009. PALSAR radiometric and geometric calibration. *IEEE Transactions of Geoscience and Remote Sensing*, **47**(12):3915-3932.
- Shimada, M., 2010. Ortho-rectification and slope correction of SAR data using DEM and its accuracy evaluation. *IEEE Journal of Selected Topics in Applied Earth Observations and Remote Sensing*, **3**(4):657-671.
- Small, D., 2011. Flattening gamma: Radiometric terrain correction for SAR imagery. *IEEE Transactions of Geoscience and Remote Sensing*, **49**(8):3081-3093.